The Role of the Medial Prefrontal Cortex in Spatial Margin of Safety Calculations

Song Qi (sqi@caltech.edu)
California Institute of Technology
Logan Cross
California Institute of Technology
Toby Wise
California Institute of Technology
Xin Sui
California Institute of Technology
John O'Doherty
California Institute of Technology
Dean Mobbs
Caltech

Article

Keywords: spatial margin of safety (MOS), Medial Prefrontal Cortex, Medial Prefrontal Cortex

Posted Date: February 12th, 2021

DOI: https://doi.org/10.21203/rs.3.rs-132967/v1

The Role of the Medial Prefrontal Cortex in Spatial Margin of Safety Calculations

Affiliations

Department of Humanities and Social Sciences and Computation, California Institute of Technology, 1200 E California Blvd, HSS 228–77, Pasadena, California 91125, USA.

Song Qi-1, Logan Cross-2 & Toby Wise-3, Xin Sui-4, John O'Doherty-5, Dean Mobbs-6

Contributions

S.Q. and D.M. designed the experiment. S.Q. and X.S. conducted the experiment and collected data. S.Q. analysed the data. S.Q., D.M., J.O. and L.G., and T.W. wrote the paper.

Corresponding author

Correspondence to: Song Qi-4 and Dean Mobbs-6

Abstract

Humans, like other animals, pre-empt danger by moving to locations that maximize their success at escaping future threats. We test the idea that spatial margin of safety (MOS) decisions, a form of pre-emptive avoidance, results in participants placing themselves closer to safer locations when facing more unpredictable threats. Using multivariate pattern analysis on fMRI data collected while subjects engaged in MOS decisions with varying attack location predictability, we show that while the hippocampus encodes MOS decisions across all types of threat, a vmPFC anterior-posterior gradient tracked threat predictability. The posterior vmPFC encoded for more unpredictable threat and showed functional coupling with the amygdala and hippocampus. Conversely, the anterior vmPFC was more active for the more predictable attacks and showed coupling with the striatum. Our findings suggest that when pre-empting danger, the anterior vmPFC may provide a safety signal, possibly via predictable outcomes, while the posterior vmPFC drives prospective danger signals.

Introduction

Staying in close proximity to safety is a key antipredator behavior as it increases the likelihood of the organism's future escape success (Mobbs et al., 2020). One metric used by behavioral ecologists to measure this safety behavior is called spatial margin of safety, where prey will adopt locations that prevent lethal predatory attack (Lima, 1985; Martindale, 1982; Wetterer, 1989) . In turn, this provides the prey with a safety net, while also reducing stress, energy consumption and promotes increased focus on other survival behaviors, such as foraging and copulation. Humans appear to use safety distance in similar ways. For example, when human subjects are placed close to a safety exit, measures of fear decrease and when under threat, and the sight of safety signals reduces fear and fear reinstatement (Christianson et al., 2008, 2011; Eisenberger et al., 2011). Here , we test the idea that when subjects are pre-empting threats of varying attack location probabilities, subjects will vary their spatial margin of safety (MOS) decisions depending on predictability. We propose that MOS decisions involve prospective spatial planning, which involves estimating safety by calculating the predator's attack locations (Cooper and Blumstein, 2015) . Further, we examine how pre-emptive MOS decisions are instantiated in human defensive circuits (Mobbs and LeDoux, 2018; Mobbs et al., 2018).

In the natural world, prey encounter predators that attack with varying degrees of uncertainty. Uncertainty is often determined by the likelihood of attack and the distribution of distances at which the threat will attack. For example, uncertainty alerts the prey that information about the predator's impending attack location is unknown, thereby resulting in increased anxiety and movement towards safety (Grupe and Nitschke, 2013). Thus, pre-empting predation via close spatial MOS, safeguards against the unpredictable spatial and temporal movements of the predator (Ii and Lima, 2006) . Consequently, the ability to predict a predator's attack location will in turn shape the prey's MOS calculations, whereby uncertain threats will result in low risk behaviors and smaller spatial radius from a refuge at the expense of forgoing other survival needs (e.g. food). In particular, frequent and salient outlier information in a given information, as presented as leptokurtic noise, makes organisms prone to overreaction and inaccurate estimations of the environment (d'Acremont and Bossaerts, 2016). Therefore, our second

question is how statistical uncertainty of a threat's attack location sways spatial MOS decisions and shifts activity in the human defensive circuits.

The prospective nature of MOS decisions may elicit activity in a set of neural circuits involved in anxiety (Adhikari, 2014) , which can be defined as a future oriented emotional state and involves the behavioral avoidance of potential dangers. Two drivers in this spatial avoidance are the ventromedial prefrontal cortex (vmPFC), and the hippocampus (Adhikari, 2014; LeDoux and Pine, 2016; Mobbs, 2018; Qi et al., 2018) (Adhikari, 2014; LeDoux and Pine, 2016) . For example, the hippocampus plays a key role in anxiety, and guides decisions via memory and prospection(Benoit et al., 2014; Hassabis et al., 2007). Further, synchronization between the hippocampus and vmPFC are associated with anxiety like behaviors(Adhikari et al., 2010; Fung et al., 2019; Padilla-Coreano et al., 2016), suggesting that the hippocampus, potentially along with the amygdala, is involved in signaling the threat significance of a stimulus. The vmPFC is a heterogeneous structure involved in information seeking, anticipation and the organization of defensive and safety responses (Adhikari et al., 2010; Dixon et al., 2017; Iigaya et al., 2019; Wallis et al., 2017). Research has shown that a safety stimulus during an aversive experience results in increased activity in the anterior vmPFC while decreasing threat also results in increased activity in the same region, suggesting that the anterior vmPFC may emit safety signals(Åhs et al., 2015; Eisenberger et al., 2011). Research also shows that attention set to safety signals, extinction, and down-regulation of anxiety are associated with vmPFC activity, suggesting that it is a key node in what has been called the fear suppression circuit(Sangha et al., 2020; Wilkinson et al., 1998; Xu et al., 2016). Conversely, the posterior vmPFC, encompassing the subgenual and rostral anterior cingulate cortex (sgACC and rACC), receives dense projections from the amygdala (Amaral and Insausti, 1992) and is implicated in negative affective responses and behavioral expression of fear(Grupe and Nitschke, 2013; Mobbs, 2018; Mobbs et al., 2007, 2010). How these, and other brain regions are evoked during pre-emptive MOS decisions is yet to be tested.

To address these gaps in knowledge between spatial MOS decisions and human defensive circuits, we created a task to investigate spatial MOS decisions under uncertainty and elucidate: (i) How do

changes in the threat's attack predictability, threat intensity, and reward value impact the subjects' MOS decisions? And ii) Do the hippocampus and vmPFC encode characteristics of threats that are central to MOS decisions? This task models the ecological phenomena where animals venture further away from their safety refuge to acquire adequate supplies of food. To create less predictable attack positions, we used leptokurtic distributions, which are evolutionarily novel and volatile in nature, and have been shown to increase the level of uncertainty and difficulty to learn to the environment (d'Acremont and Bossaerts, 2016). Leptokurtic noise is generated as the composite of two normal distributions with similar means and contrasting variances. Leptokurtic distributions are thus probability density curves that have higher peaks at the mean and are fatter tailed where extreme outcomes (outliers) are expected more (Fig. C). We contrasted this with standard Gaussians (Fig. 1D and E)), which are more computationally familiar. We hypothesized that when subjects are facing virtual predators with higher frequency of outlier attack distributions, this will result in more uncertainty and therefore, decisions to move closer to safety.

Fig. 1: Experimental Structure

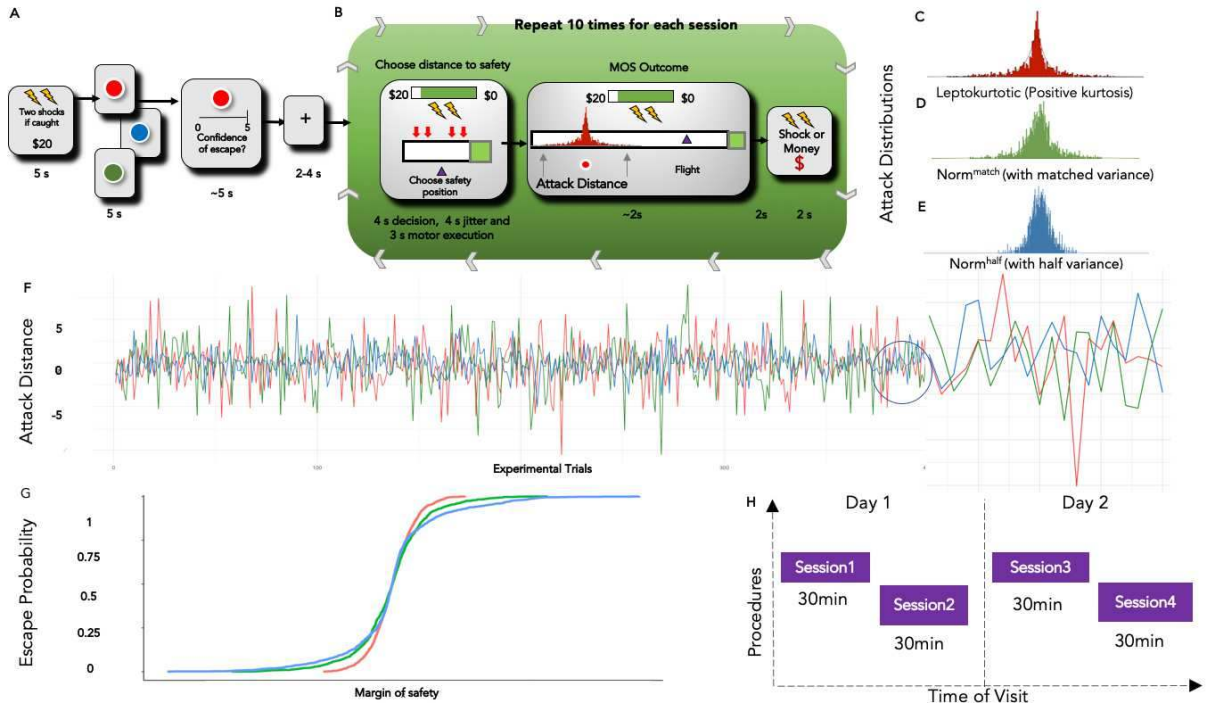

(A)During the MOS decision task, every 10 trials are grouped as a block. Participants were first presented with a screen with a series of information at the beginning of every block, including the reward/shock level, color of the predator (leptokurtic condition in color red; normmatch in color green, where the variance of the distribution is matched with the leptokurtic condition.; normhalf , in color blue, where the variance is half as compared to the leptokurtic condition). Next, they were asked to rate how confident they were to escape the threat from a scale of 1 to 5. Participants were then presented with information regarding shock and reward levels. There are 4 conditions in total : low reward, low shock, where one shock and the base reward is administrated; low reward, high shock, where two shocks and the base reward is administrated; high reward, low shock, where one shock and twice the base reward is administrated; high reward, high shock, where two shocks and twice the base reward is administrated. (B) During a trial, for the first 4 seconds, participants were presented with a screen displaying the margin of safety runway and their initial location. They were told to make a choice of which runway position they want to be at when the threat approaches later. To prevent motor confounds, they were specifically told to only mentally make the decision, and blocked from pressing the button during this phase. After a 4-second jitter, they were presented with the same screen again where they can press the button and move to the desired MOS location. A dynamic bar displaying the maximum possible reward associated with the chosen MOS location is also presented on top of the screen. In the next 2 seconds, the outcome of the chasing was revealed, including whether their escape was successful and how much reward was gained. Attack distributions for (C)leptokurtic distribution ; (D) gaussian distribution with matched variance and (E) half the variance gaussian; (F) the predator's attack distances through all trials. Zero on the Y axis marks the mean of the distribution, while numbers represent how far away the drawn instance is away from the mean. (G) Escape probability. X axis represents possible margin of safety choices, while Y access represents the corresponding probability of escape. (H) Schematic representation of the experimental procedure. Participants undergo 4 x 30 min scans sessions over a two-day period.

Results

Participants make less risky MOS choices in the less predictable threat environment

MOS choice in the task represents the position participants selected relative to the safety refuge. A position choices that is closer to the safety is considered less risky, granting participants an easier access to the exit. In order to investigate how the uncertainty of predator attacks modulate MOS choices, we first examined how MOS decisions vary across distributions types, with a repeated-measures, one-way ANOVA. The result showed a main effect of distribution type [$F(2,44) = 61.33$, $p < 0.001$]. A Tukey post hoc test revealed that participants' MOS choices were significantly closer to the safety zone in the leptokurtic distribution condition (0.74 +- 0.06) than in the normmatch condition (0.68 +- 0.03) and normhalf condition (0.67 +- 0.01). This indicates that participants made less risky MOS choices in a less predictable threat environment, potentially as a result of their perceiving the leptokurtic attackers as more dangerous. Interestingly, there was no significant difference in mean MOS choices between the two normal distributions. This suggests a mere difference in attack distance variance is not sufficient to drive behavioral change. (Figure 2 a,b,c,d)

Fig. 2: Behavioral Results

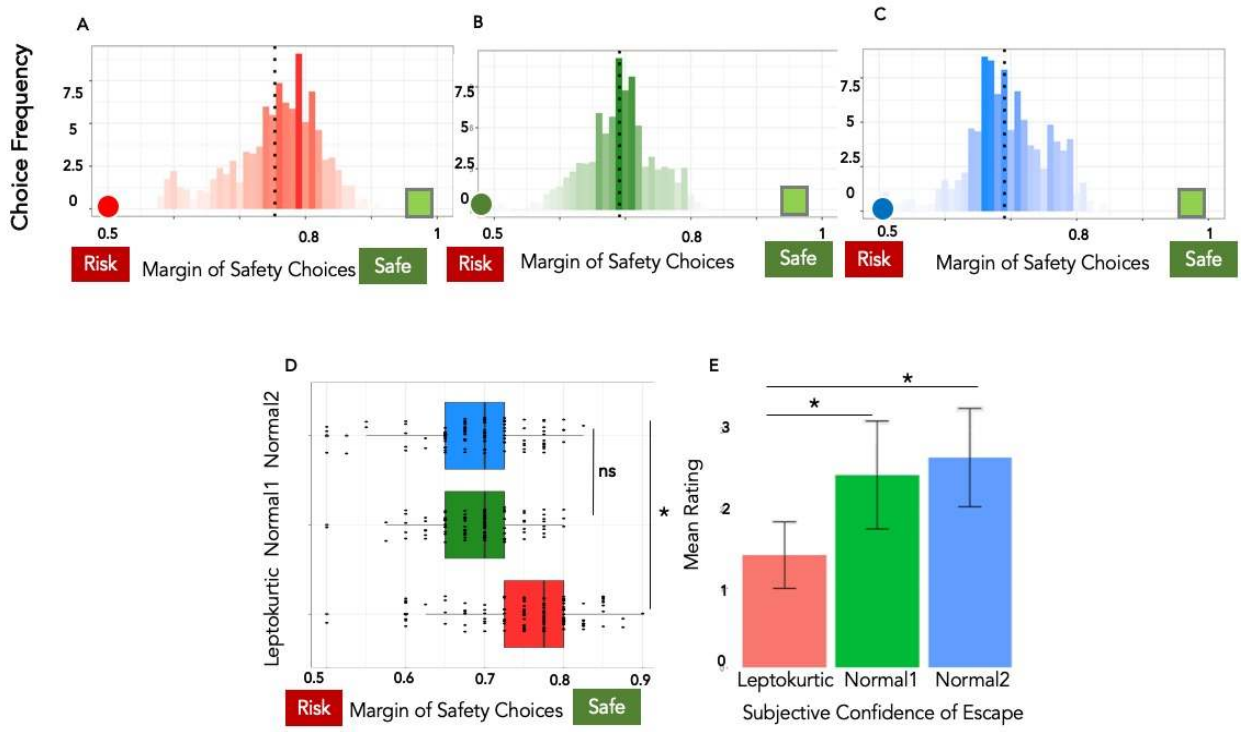

Choice frequencies for (A) leptokurtic, (B) matched variance normal and (C) half variance normal attacking threats. The MOS decision phase and the outcome. (D): Confidence ratings for leptokurtic distribution, matched variance normal distribution, and normal distribution with half variance. Post-hoc analysis revealed that participants were less confident in the leptokurtic condition compared to the other two conditions ($p < 0.001$). Leptokurtic attack location are in red; normal distribution with matching variance are in green; and normal distribution with half variance are in blue.

Participants made less risky MOS choicesin threat environment with higher punishment

To further disentangle how shock and reward levels could interact with predator attack type as additional external incentives, we examined participants' MOS choices within different shock and reward conditions. While there was no significant difference in their MOS decisions when facing different levels

of rewards ($t(21) = 1.378$, $p = 0.182$) their MOS choices were significantly less riskt in the high shock condition (0.75 +- 0.07), compared to the low shock condition (0.69+-0.05): $t(21) = 21.21$, $p < 0.001$. This suggests that participants were sensitive to the level of danger and adjusted their MOS decisions accordingly (Supplementary figure 1). The lack of sensitivity to rewards comes potentially from the overwhelming aversiveness of the shock. (1)

More confident participants made riskier MOS decisions

Having shown that the level of predictability in the attack distribution influences MOS decisions, we asked whether it also affects subjective confidence in escape success. We collected participants' confidence ratings before every unique trial block (shown in figure 1 A/B, where every 10 trials consist a unique trial block). An ANOVA on the confidence ratings also revealed that participants were generally more confident on trials in the normal distributions (both matched variance and half variance) compared with trials in the leptokurtic distribution. A main effect of distribution type was found [$F(2,44) = 27.32$, $p < 0.001$], and a Tukey post hoc test showed that confidence rating in the leptokurtic condition (1.42 +- 0.42) was significantly lower than those in the normmatch condition (2.43 +- 0.68) and the normhalf variance (2.65 +- 0.62) ($p < 0.001$) (figure 2 e). We also examined the relationship between participants' MOS choices and confidence ratings. Interestingly, a significant correlation was only observed in the leptokurtic condition, where individuals who were more confident made riskier MOS choices ($r = -0.54$. $p = 0.04$). This effect was not observed for either the normmatch condition ($r = 0.25$, $p = 0.37$) nor the normhalf condition ($r = -0.31$, $p = 0.27$).

MOS decisions are represented within prefrontal and subcortical regions

Building on our behavioral results, we next sought to identify neural systems underlying MOS decisions in response to varying levels of threat predictability. Due to the design feature of the behavioral experiment, the decision phase consists of both a cognitive (perception of the threat) and decision

component, making the univariate analysis insufficient to capture the underlying dynamics of the neural process (Davis et al., 2014; Norman et al., 2006). The MVPA analysis here thus serves two main purposes: 1) to identify the key regions involved in decision making under the current threat, and 2) to distinguish the underlying neural mechanism among threats with different levels of predictability. Results of this analysis can then be used to inform ROIs for subsequent connectivity and parametric modulation analysis. To accomplish this, we used a searchlight cross-decoding approach using linear support vector regression (SVR) and leave-one-out cross-validation (see Supplementary Methods).

Two separate whole brain searchlight analysis were performed to answer the following questions respectively: which regions are critically involved in 1) perceiving different attacking distributions and 2) making Margin of safety choices. Admittedly, there are potential overlap between the threat perception and decision making process. But our aim here is to identify the critical regions separately to better understand the processing stream.

The first classifier predicted which attacking distribution a given trial belonged to. This showed that regions including the right insula and the mid-cingulate cortex (MCC) encoded the distribution type, with a decoding accuracy significantly higher than the Monte-Carlo simulated chance level accuracy (overall accuracy: $t(21) = 2.82$, $p = .010$). The whole brain decoding map was thresholded at $P<0.05$ (FWE) (Fig. 3a).

Next, for the analysis of MOS decision types, each trial was labelled according to the MOS decision the participant made, and a classifier was trained to predict which trials fall into which decision categories. The categories were created by grouping MOS choices that are close in spatial distance together. During the task, the entire MOS choice runway is divided to 6 segments from left to right, resulting in 6 MOS decision categories. Each choice category thus represents a level of how close participants place themselves to the safety. Decoding of choices was found in regions including the right hippocampus,

vmPFCpost and vmPFCant with a decoding accuracy significantly higher than chance level ($t(21) = 2.47$, $p = .022$). These results suggested that the both the distribution type and MOS decision making process is robustly represented in the above mentioned prefrontal and subcortical regions. (Fig. 3 A,B)

Fig. 3: Neural representation of pre-emptive MOS decisions.

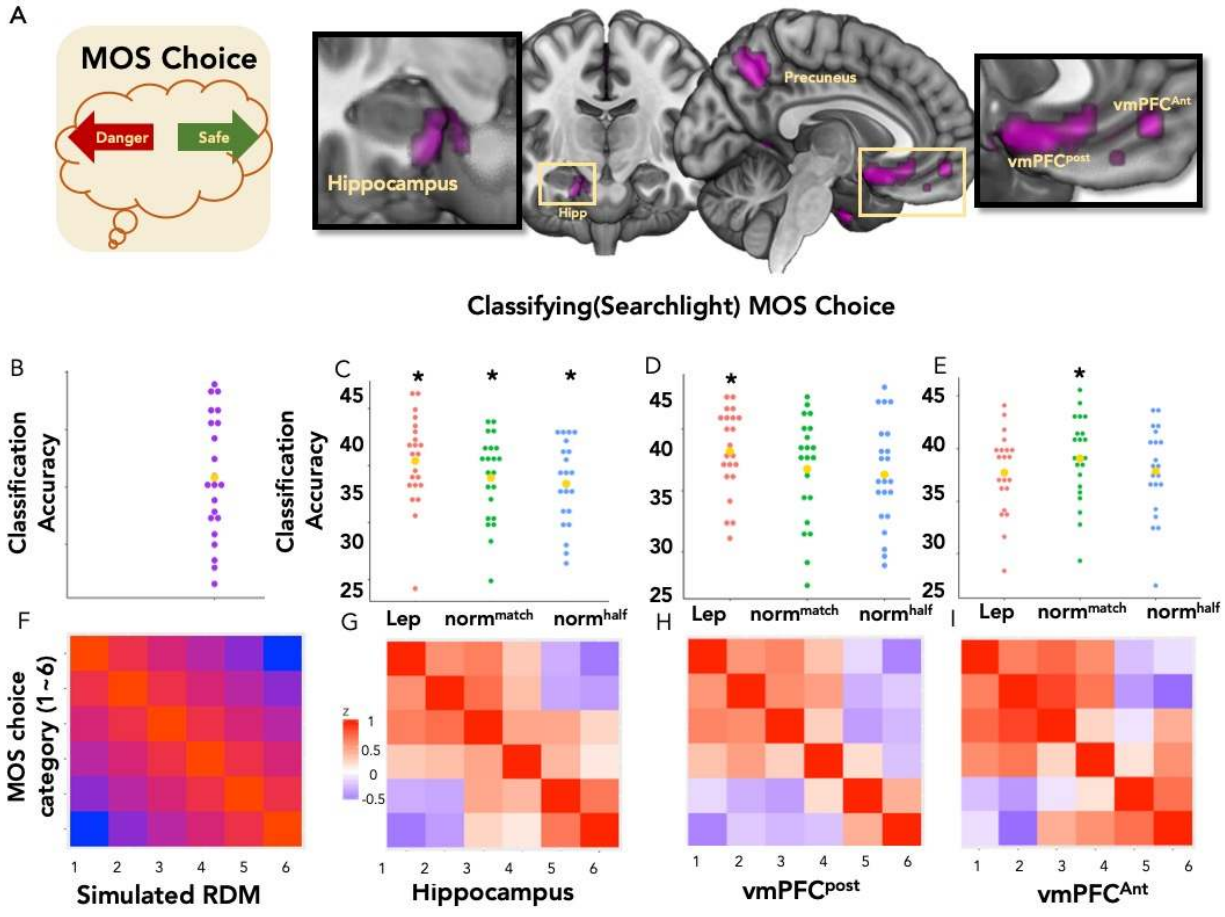

Avoidance decisions decoded in the vmPFC and the Hippocampus. (A): whole brain searchlight map displaying statistically significant regions for the MOS choice classifier (FDR corrected, $p < 0.05$). (B): Classification accuracy of the MOS choice classifier. Each dot represents data from a single participant. Average accuracy was significantly higher than the simulated chance level ($p < 0.001$). Box and whisker plots display accuracies from the region of interest classifiers, targeted at the pre-defined ROIs (the hippocampus, vmPFC (posterior) and vmPFC (anterior)).(C): In the hippocampus, classification accuracy from all three attack conditions were significantly higher than their corresponding chance levels. (D); Classification accuracy was only significantly higher than the chance level in the leptokurtic distribution

in vmPFCpost .(E): Classification accuracy was only significantly higher than the chance level in the normmatch condition in vmPFCant . (F): Behavioral similarity structure among MOS choices. The Behavioral similarity structure displays how similar MOS choices are at the behavior level. For example, MOS choice 1 and 2 are closer in distance compare to choice 1 and 6, thus more similar in the structure. Naturally, choices are more similar when in close spatial distance, and more dissimilar when in sparse spatial distance. (G): Actual pattern similarity within the regions of interest. The neural RDM in the hippocampus was significantly correlated with the theoretical model ($r = 0.593$, $P < 0.001$). Similar correlation effects were also found in (H) vmPFCpost and (I) vmPFCant, ($r = 0.754$, $p < 0.001$; $r = 0.482$. $p < 0.001$).

vmPFC subregions differentially encode MOS decisions according to levels of predictability

The regions implicated in the whole brain searchlight overlap with ROIs in previous literature shown to be critically involved in the process of decision making under threat. We thus performed MVPA analysis within each ROI, namely the hippocampus, vmPFCpost and vmPFCant to investigate how they uniquely contributed to the MOS decision process. Within each specified ROI, we investigated classification accuracy for the MOS decisions labels, separately for each distribution conditions. Thus, by comparing how well the process is decoded within each ROI, we can examine how the involved regions drive behavioral change depending on the levels of predictability in different attacking conditions.

Within the vmPFCpos , only choice decoding for the leptokurtic condition was significantly above the Monte-Carlo simulated chance level (Monte-Carlo simulated baselines: leptokurtic, 36.7%; normmatch , 34.8%; normhalf, 33.7%) (leptokurtic distribution, $p < .001$; normmatch, $p = .410$; normhalf, $p = .868$). Within the vmPFCant, only classification for the normmatch condition was significantly above chance level (leptokurtic distribution, $p = .341$; normmatch, $p = .004$; normhalf, $p = .156$). Within the

hippocampus, classification for all 3 distribution types was significantly above chance level (leptokurtic distribution, $p < .001$; normmatch, $p = .011$; normhalf, $p = .038$). A follow up ANOVA did not reveal a significant difference among the decoding accuracies (Fig. 3 B,C,D,E).

Univariate overlap with vmPFC regions involved in 'fear' and 'extinction'

To validate the functionality of brain regions identified as vital within the MOS paradigm, we constructed ROIs from neurosynth using the key words "fear" (for comparison with posterior vmPFC/sgACC) and "extinction" (for comparison with vmPFCant) . ROIs were constructed using 6mm spheres from the peak coordinate. The above comparisons were made because we hypothesized that the two pairs of concepts would overlap: 1) "fear" and the approaching/increment of threat; 2) "extinction" and the reduced level of threat. We then performed SVC with the "fear" ROI on vmPFCpos with the leptokurtic contrast ($p < 0.001$, $T = 5.07$, cluster size = 31, (0,26,-12)) and SVC with the "extinction" ROI on vmPFCant ($p = 0.010$, $T = 4.35$, cluster size = =11, (-2,46,-10)). For a full list of activated regions, please refer to supplementary table 1. These coordinates overlap with the corresponding ROIs taken from the searchlight analysis, indicating that information processing and learning through both fear and safety are potentially presented in MOS decision making through vmPFCpost and vmPFCant, respectively.

vmPFC activity encodes MOS decisions

Having demonstrated that vmPFC activity patterns encode MOS decisions, the next step was to ask whether overall BOLD activity levels in the vmPFC also covaried with MOS decision (Fig. 4E). To test this, we constructed two univariate parametric modulators indicating whether the participants' final MOS choices is a safety choice or a risky choice (compared to their randomly assigned initial location). The parametric modulation of univariate data thus reveals what regions showed activity associated with risky/safety choices under different levels of predictability. Inspection of the resulting statistical maps, using SVCs from the previously constructed vmPFCpost and vmPFCant ROIs, showed that the "move to

danger" and "move to safety" modulations were significant in the vmPFCpost and vmPFCant ROIs respectively (Move to danger: $p < 0.001$, $T = 6.44$; Move to safety: $p < 0.001$, $T = 4.39$, supplementary table 4).

vmPFC activity encodes MOS decisions

Having demonstrated that vmPFC activity patterns encode MOS decisions, the next step was to ask whether overall BOLD activity levels in the vmPFC also covaried with MOS decision (Fig. 4E). To test this, we constructed two univariate parametric modulators indicating whether the participants' final MOS choices is a safety choice or a risky choice (compared to their randomly assigned initial location). The parametric modulation of univariate data thus reveals what regions showed activity associated with risky/safety choices under different levels of predictability. Inspection of the resulting statistical maps, using SVCs from the previously constructed vmPFCpost and vmPFCant ROIs, showed that the "move to danger" and "move to safety" modulations were significant in the vmPFCpost and vmPFCant ROIs respectively (Move to danger: $p < 0.001$, $T = 6.44$; Move to safety: $p < 0.001$, $T = 4.39$, supplementary table 4).

Representational similarity analysis of the vmPFCpost, vmPFCant and hippocampus

The MVPA searchlight analysis offers insights into key regions involved in encoding the MOS decision process. However, it is left unclear how different MOS choices (in this case, choices within one of the choice categories) were neurally represented in the ROIs. Thus, we conducted a representational similarity analysis to investigate the underlying geometry of the neural encoding of the MOS decision variables in the ROIs. Distinctive clustering in the RDM structure also help further validate the original behavioral paradigm, showing how sensitive participants were to all the possible MOS choice categories.

A Behavioral RDM, together with RDMs from the neural data within the hippocampus, vmPFCpost, and vmPFCant were constructed to investigate the potential MOS decision information and perceived distribution information embedded in the activity patterns of these ROIs. A high level of similarity between the theoretical structure (behavioral RDM) and the actual brain activity (neural RDM) in a certain ROI will indicate that task-relevant information is encoded in a way that is consistent with the behavioral structure of the during the MOS decision process. Figure 3 illustrates the theoretical/behavioral RDMs constructed by the pairwise relations of the 6 MOS decision categories. Spearman correlation coefficients were used to calculate the distance between the model and neural data matrices. The neural RDM in the hippocampus was significantly correlated with the theoretical model ($r = 0.593$, $P < 0.001$) across all conditions. Similar correlation effects were also found in vmPFCpost and vmPFCant, ($r = 0.754$, $p < 0.001$; $r = 0.482$. $p < 0.001$), but these were specific to the leptokurtic and normmatch conditions respectively (fig 3f,g,h,i).

Converging evidence from the searchlight analysis, univariate parametric modulation, and RSA analysis has shown that the vmPFC subregions (vmPFCpost and vmPFCant) play a vital role in the encoding of MOS decisions under environments with different levels of predictability. Next,we further investigate the connectivity structure seeding from these regions.

Fig. 4: Psychophysiological interactions seeding from regions of interest and meta analytical decoding

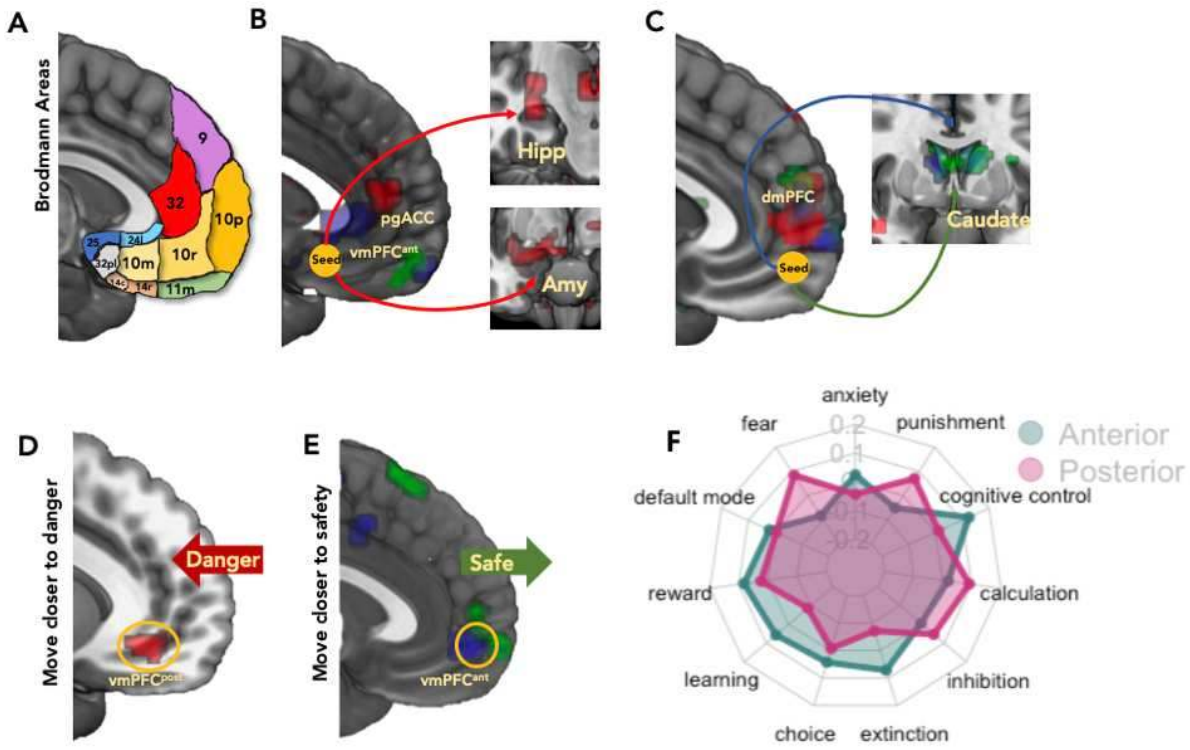

312

313 (A) Example of Brodmann Areas (BA) that distinguish posterior-anterior axis. For example, the posterior
314 vmPFC reflects BA 25, 24, 32(ACC), 10m and 14, while the anterior encompasses BA 10p, 10 r 11, and 32
315 (non-ACC). This is made clearer by the dotted line. Connectivity analysis were first performed on the
316 anterior and posterior vmPFC seeds, where 6 mm spheres centered on the peak voxel of the
317 corresponding clusters in the MVPA searchlight were used as seeding regions. (B) For the posterior
318 vmPFC seed, in all three attacking conditions, the connectivity maps showed significant connectivity
319 between the hippocampus and the seeding region (leptokurtic: $p < 0.001, T = 4.06$; normmatch: $p <$
320 $0.001, T = 3.62$; normhalf : $p = 0.011, T = 3.18$). Interestingly, only in the leptokurtic attacking condition,
321 the amygdala was found significant on the connectivity map ($p < 0.001, T = 4.60$). (C) On the other hand,
322 with the anterior vmPFC seed, all three attacking conditions showed significant connectivity towards the
323 Caudate (leptokuctic: $p < 0.001, T = 3.87$; normmatch $P < 0.001, T = 4.23$; normhalf $P < 0.001, T =$
324 4.59.). We constructed two parametric modulators indicating whether the participants' final MOS

choices is a (D) safety choice or a (E) risky choice (compared to their randomly assigned initial location). The parametric modulation of univariate data thus reveals what regions were associated with risky/safety choices under different levels of predictability. On the resulting statistical maps, using SVCs from the previously constructed vmPFCpost and vmPFCant ROIs, we found that the "move to danger" and "move to safety" modulations were significant in the vmPFCpost and vmPFCant ROIs respectively (Move to danger: $p < 0.001$, $T = 6.44$; Move to safety: $p < 0.001$, $T = 4.39$) (F) Meta-analytical decoding with Neurosynth. Red and Green radar bars represent correlation strength between key words and the anterior ($x = 0$, $y = 26$, $z = -12$) and posterior($x = -2$, $y = 46$, $z = -10$) vmPFC ROIs.

Differences in vmPFC subregion connectivities

With vmPFCpost and vmPFCant identified as key regions associated with risky and dangerous choices, we were interested in how these regions regulate MOS decisions in concert with subcortical structures. To test this, we performed connectivity analysis using gPPI (see supplementary methods), to reveal regions that showed covarying activity with our vmPFC seed regions. From the MVPA analysis, we took the vmPFCpost and vmPFCant as seed regions for the leptokurtic distribution contrast and normal distribution contrasts, since they were identified as regions representing the process where participants make risk decisions under the corresponding predator conditions. PPI analyses were first performed on the moving to safety/danger contrast, respectively on the vmPFCpost and vmPFCant, ROIs (fig 4 b c) For the vmPFCpost seed, in all three attacking conditions, the connectivity maps showed significant activation in the hippocampus (leptokurtic: $p < 0.001$,$T = 4.06$; normmatch: $p < 0.001$, $T = 3.62$; normhalf : $p = 0.011$, $T = 3.18$). Interestingly, only in the leptokurtic attacking condition did the amygdala show significant coupling with the vmPFCpost ($p < 0.001$, $T = 4.60$). On the other hand, with the anterior vmPFC seed, all three attacking conditions showed significant connectivity towards the caudate (leptokurtic: $p < 0.001$,$T = 3.87$; normmatch $P < 0.001$, $T = 4.23$; normhalf $P < 0.001$, $T = 4.59$.). For a full list of activated regions, please refer to supplementary table 2.

Subjects continually optimize MOS decisions through adaptive learning from trial outcomes

In order to perform effectively on the task, subjects may continually adjust their policy depending on their perceived likelihood of escape which is updated on every trial depending on its outcome. We sought to test this by fitting a simple reinforcement learning model to the behavioral data which assumes subjects estimate the likelihood of receiving a given reward (which depends on both the available reward level and the likelihood of survival) on each trial.

This took the form of a standard Rescorla-Wagner learning model which was used to characterize participants' margin of safety choice behaviors. The learning rate 'α' reflects to what extent participants' choice of MOS is based on the most recent outcomes. A high learning rate indicates that choice behavior is updated in a more rapid manner based on the difference between the expected choice outcome and the actual choice outcome. In contrast, at low learning rates, surprising outcomes lead to little change in their choice on the next trial. In the current study, we estimated participants' learning rates in the uncertain vs more certain attack position blocks by fitting a reinforcement learning model(Browning et al., 2015) to their choices in each task block (10 trials per session, as described in figure 1).

We first examined whether our model recapitulated observed patterns in the MOS decision data. The model demonstrated behavior that was consistent with the true data (Figure 5 a), indicating that a reinforcement learning model can describe subjects' behavior in the task. We next assessed whether participants, as a group, adapted their learning rate in response to the change in attack distances between the more predictable normal distributed attack distances and more uncertain attack distances characterized by leptokurtic outliers. Consistent with previous studies of reinforcement learning, participants' learning rates were higher in the leptokurtic attack than the more predictable normally distributed attacks positions. (Main effect of attack distribution: $F(2,63) = 4.43$, $p = 0.0159$. Post hoc comparisons, $p<0.001$)

(figure 5 b), indicating that subjects adapted their learning based on the level of uncertainty in the attack distribution.

MOS prediction errors are tracked by a distributed network of brain regions

A parametric modulation analysis on univariate data, using the prediction error from the RL model was performed to address what underlying neural processes were involved during the learning process of participants' MOS decisions. Small volume corrections were performed on the key ROIs : hippocampus: leptokurtic: $p = 0.002$; normmatch: $p = 0.004$; normhalf: $p = 0.191$; amygdala: leptokurtic: $P = 0.014$; normmatch: $p = 0.006$; normhalf: $P = 0.094$; striatum: leptokurtic: $p < 0.001$; normmatch: $p < 0.001$; normhalf: $p < 0.001$. This suggests that while the striatum decodes the representation of prediction error in all three attacking distributions, the hippocampus and amygdala were involved only in the leptokurtic and normmatch attacking conditions. (figure 5 d e).

Fig. 5: Behavioral modelling

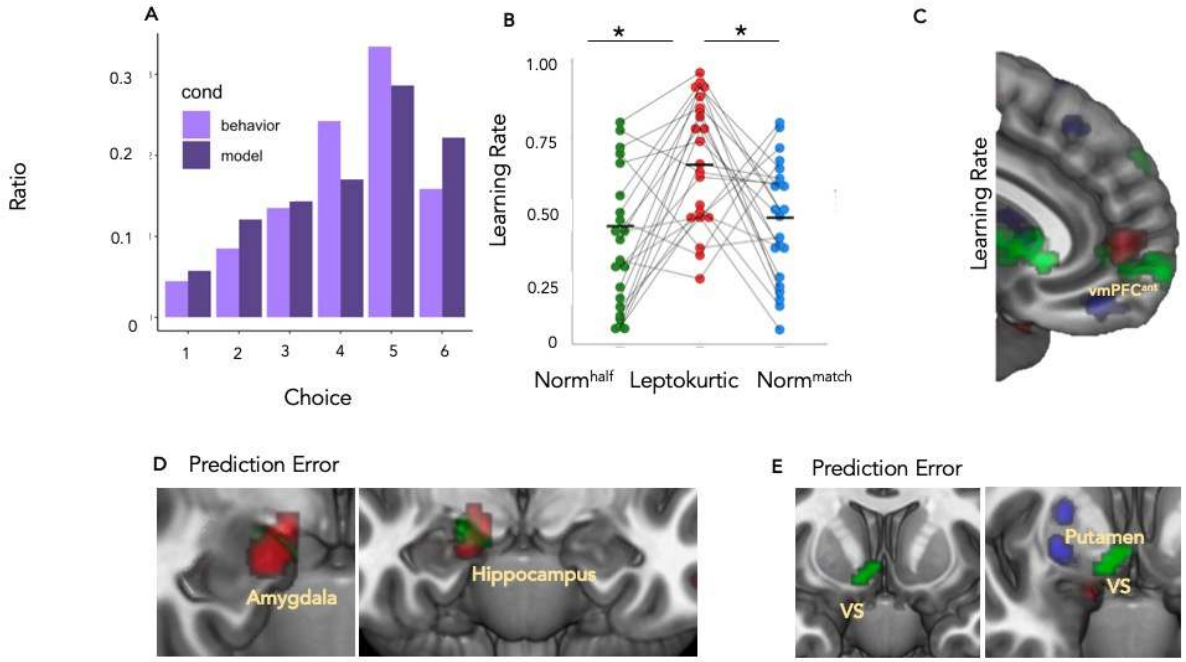

(A) Actual MOS choice categories and model fitting MOS choice categories. Choice 1~6 are choice categories from risky to safe. Y axis represents the choice ratio under each category (B) Learning rate from the reinforcement learning model over two days. Data of two sessions within one day were averaged across participants. Learning rate in the leptokurtic condition (which is more predictable) was significantly higher than the other two conditions (posthoc $p < 0.001$).(C): Maps showing parametric modulation with prediction errors from the model. Small volume corrections (D): (hippocampus): leptokurtic: $p = 0.002$,; norm1: $p = 0.004$; norm2: $p = 0.191$; (amygdala): leptokurtic: $P = 0.014$; norm1: $p = 0.006$; norm2: $P = 0.094$ (E): (striatum): leptokurtic: $p < 0.001$; norm1: $p < 0.001$; norm2: $p < 0.001$. For the remaining activated regions, please refer to supplementary table 3.

Discussion

We found evidence in support of our hypothesis that in uncertain environments, participants adjust their distance to be closer to safety(Mobbs et al., 2015). We also show that when encountering a more uncertain threat, participants decreased confidence in escape success, while displaying higher learning rates, signifying that under uncertain environments, people adjust decisions more based on recent, immediate information, instead of accumulated information over time. Our MVPA analysis shows that the vmPFCPost is associated with avoidance of more uncertain threats and consequently the decision to stay closer to safety. The vmPFCPost also showed increased functional coupling with the hippocampus and amygdala, supporting the known connectivity with this region as well as its role in control of fear(Mobbs and Kim, 2015; Nili et al., 2010). On the other hand, the vmPFCAnt was associated with more certain attack locations and thereby executing safer decisions. These results are congruent with the idea that vmPFC sub-regions play distinct roles in both danger and safety signals that reflect the ability to predict positive or negative outcomes with a threat.

Our results suggest that when the attack location is relatively predictable (i.e. normmatch and normhalf Gaussian distributions), participants make more risky MOS choices. That is, subjects choose to place themselves further away from the safety exit to earn more reward. On the other hand, when the attack location is more unpredictable (i.e. leptokurtic distribution), participants tended to place themselves closer to safety and thus displayed more protective actions. Critically, despite significant differences in variance, there were no differences in MOS decisions between the two Guassian distributions. This suggests that participants' decision patterns facing uncertain threats was not swayed by a simple change in distribution variance, but by a total structural change in the predictability of the distribution. This was echoed in participants' subjective rating of their confidence, a reflection of how likely they felt they were to escape (Fig. 2E).

When dissecting the defensive circuitry, it is critical to understand which brain regions are involved in the avoidance of forthcoming danger. Our MVPA searchlight identified three key regions, namely the hippocampus, the vmPFCPost and the vmPFCAnt. Interestingly, when looking at the classification accuracies, we found that within the vmPFCAnt, classification accuracy was above chance level only for the normhalf, in line with our prediction that this region would be involved in the most more predictable attack locations. On the other hand, within the vmPFCPost, the classification was more accurate than chance level only for the more unpredictable, leptokurtic distribution condition. This suggests a separation of vmPFC subregions in terms of functional roles. While the vmPFCAnt is correlated with more predictable decision environments, the vmPFCPost seems to be associated with more volatile counterparts. Interestingly, the hippocampus classification accuracies revealed no differences between attack locations distributions, suggesting a more general role in avoidance decisions.

The vmPFCPost may function as a hub when the environment is more uncertain and where more information gathering is needed. Further evidence for this comes from our parametric modulation analysis using relative MOS from the starting position, which showed that more dangerous choices are associated with activation in the vmPFCPost. This suggests a tentative role for the vmPFCPost to be responsible for computations concerning a more unpredictable environment, or a more risky choice. In our connectivity analysis seeding from the vmPFCPost, we observed activations in amygdala and hippocampus only in the uncertain attacking locations. Previous research has shown a role for the amygdala-mPFC as a pathway of modulating threat avoidance behavior, and hippocampus as a center for representing predictive relationships between environmental states (Lisman and Redish, 2009; Stachenfeld et al., 2017). This is in line with the idea that for decision making under threat with less predictability, more predictive computations are required.

The vmPFCAnt modulates behavior when the environment is relatively easy to predict during the spatial MOS decisions. Interestingly, using relative MOS from the starting position as a modulator in the parametric modulation analysis, the vmPFCAnt was also activated when the choice is categorized as "safe". In previous studies, this region has been implicated in both safety learning through extinction and safety learning through active avoidance (Eisenberger et al., 2011; Harrison et al., 2017). For example, studies using the lever press avoidance task in rodents have shown activation of the prelimbic regions of MPFC (the rodent homologue of human anterior vmPFC) during the expression of active avoidance(Bravo-Rivera et al., 2015; Diehl et al., 2018) . These regions partially overlap with the identified clusters of vmPFCAnt in our task. Further, when looking at functional connectivity seeding from the vmPFCAnt, the caudate was significant only in the two more predictable predator conditions, although there may be other explanations (action selection(Lau and Glimcher, 2007)). This resonates with previous studies where vmPFC not only functions as a center for signaling safety, but also in reward related processes, because safety processing may be "intrinsically rewarding or reinforcing" (Eisenberger

et al., 2011) . This is also supported by a parametric modulation analysis showing that shifts towards safety activate the vmPFCAnt. Also involved in this process is the striatum, which has been shown to be responsible for fear memory extinction(Alexander et al., 2019; Maren and Quirk, 2004). For example, previous research on rodents has shown that in rats, the dopamine level in the striatum was unchanged after exposure to novel environmental stimulus, but follows more closely to the expression of conditioned response(Wilkinson et al., 1998). Interestingly, this orchestrates with our finding where the striatum is only responsive to the high predictability threats together with the vmPFCAnt.

We further correlated the neural data with behavioral parameters from the exploratory reinforcement learning model. Parametric modulation using prediction error from the RL model also activated the amygdala in the more uncertain, leptokurtic attacking condition, providing additional evidence for the modulation mechanism where amygdala is involved in the more volatile threat conditions when large discrepancies between expected and observed outcomes happen. Within all predator conditions, the ventral striatum and putamen were also significantly activated in correlation with the PE signal. This is consistent with previous studies where learning under uncertain environments occurs through reward based pathways(Jocham et al., 2011; Leong et al., 2017). On the other hand, parametric modulation using learning rates established vmPFCAnt as a hub for MOS decision making when facing predictable attack distances.

The hippocampus also emerged as a central region involved in MOS decisions. First, decoding of choice was higher than chance level in the hippocampus, regardless of how uncertain the attacking locations were. However, the hippocampus only showed functional connectivity with the vmPFCPost in the uncertain, leptokurtic attacking condition. The first finding resonates with the idea that the hippocampus has long been thought of as a predictive map and center for planning when considering future actions

485 based on immediate feedback from the environment (Bach et al., 2014; Lisman and Redish, 2009;
486 Stachenfeld et al., 2017). It was thus universally involved regardless of the uncertainty level of the
487 attacking environment. However, our results indicate that activity in the hippocampus becomes more
488 coordinated with the vmPFCPost in situations which require more intensive planning, as evidenced by the
489 distinct functional connectivity to the hippocampus when the subjects are encountering a more
490 unpredictable, leptokurtic, attacking threat. Indeed, our finding corresponds to previous studies using
491 rodents where the hippocampus has been shown to specifically contribute to model based planning, that
492 may include also memory based decision making (Miller et al., 2017) .

493

494 The current study offers the first insight into how spatial MOS decisions are determined in threat
495 environments with different levels of predictability. It also establishes the posterior and anterior vmPFC
496 subregions as centers modulating the push and pull between risky and safe choices, where the
497 hippocampus is involved in both processes in a more universal manner. More work is needed to further
498 validate the functional separation of vmPFC subregions in terms of their roles during decision making
499 under threat. These new insights, however, suggest a dissociable role of the vmPFC in anxiety, where the
500 vmPFCPost is involved in heightened threat signals, while the vmPFCAnt may be involved in down
501 regulation of threat via safety signals.

502 # References
503

504 1. d'Acremont, M., and Bossaerts, P. (2016). Neural Mechanisms Behind Identification of
505 Leptokurtic Noise and Adaptive Behavioral Response. Cereb. Cortex 26, 1818–1830.
506 2. Adhikari, A. (2014). Distributed circuits underlying anxiety. Front. Behav. Neurosci. 8.
507 3. Adhikari, A., Topiwala, M.A., and Gordon, J.A. (2010). Synchronized activity between the
508 ventral hippocampus and the medial prefrontal cortex during anxiety. Neuron 65, 257–269.

4. Åhs, F., Kragel, P.A., Zielinski, D.J., Brady, R., and LaBar, K.S. (2015). Medial prefrontal pathways for the contextual regulation of extinguished fear in humans. NeuroImage 122, 262–271.
5. Alexander, L., Clarke, H.F., and Roberts, A.C. (2019). A Focus on the Functions of Area 25. Brain Sci. 9, 129.
6. Amaral, D.G., and Insausti, R. (1992). Retrograde transport of D-[3H]-aspartate injected into the monkey amygdaloid complex. Exp. Brain Res. 88, 375–388.
7. Bach, D.R., Guitart-Masip, M., Packard, P.A., Miró, J., Falip, M., Fuentemilla, L., and Dolan, R.J. (2014). Human Hippocampus Arbitrates Approach-Avoidance Conflict. Curr. Biol. 24, 541–547.
8. Benoit, R.G., Szpunar, K.K., and Schacter, D.L. (2014). Ventromedial prefrontal cortex supports affective future simulation by integrating distributed knowledge. Proc. Natl. Acad. Sci. 111, 16550–16555.
9. Bravo-Rivera, C., Roman-Ortiz, C., Montesinos-Cartagena, M., and Quirk, G.J. (2015). Persistent active avoidance correlates with activity in prelimbic cortex and ventral striatum. Front. Behav. Neurosci. 9.
10. Browning, M., Behrens, T.E., Jocham, G., O'Reilly, J.X., and Bishop, S.J. (2015). Anxious individuals have difficulty learning the causal statistics of aversive environments. Nat. Neurosci. 18, 590–596.
11. Christianson, J.P., Benison, A.M., Jennings, J., Sandsmark, E.K., Amat, J., Kaufman, R.D., Baratta, M.V., Paul, E.D., Campeau, S., Watkins, L.R., et al. (2008). The Sensory Insular Cortex Mediates the Stress-Buffering Effects of Safety Signals But Not Behavioral Control. J. Neurosci. 28, 13703–13711.
12. Christianson, J.P., Jennings, J.H., Ragole, T., Flyer, J.G.N., Benison, A.M., Barth, D.S., Watkins, L.R., and Maier, S.F. (2011). Safety signals mitigate the consequences of uncontrollable stress via

a circuit involving the sensory insular cortex and bed nucleus of the stria terminalis. Biol. Psychiatry 70, 458–464.

13. Cooper, J.W.E., and Blumstein, D.T. (2015). Escaping from Predators: An Integrative View of Escape Decisions (Cambridge University Press).
14. Davis, T., LaRocque, K.F., Mumford, J.A., Norman, K.A., Wagner, A.D., and Poldrack, R.A. (2014). What do differences between multi-voxel and univariate analysis mean? How subject-, voxel-, and trial-level variance impact fMRI analysis. NeuroImage 97, 271–283.
15. Diehl, M.M., Bravo-Rivera, C., Rodriguez-Romaguera, J., Pagan-Rivera, P.A., Burgos-Robles, A., Roman-Ortiz, C., and Quirk, G.J. (2018). Active avoidance requires inhibitory signaling in the rodent prelimbic prefrontal cortex. ELife 7, e34657.
16. Dixon, M.L., Thiruchselvam, R., Todd, R., and Christoff, K. (2017). Emotion and the prefrontal cortex: An integrative review. Psychol. Bull. 143, 1033–1081.
17. Eisenberger, N.I., Master, S.L., Inagaki, T.K., Taylor, S.E., Shirinyan, D., Lieberman, M.D., and Naliboff, B.D. (2011). Attachment figures activate a safety signal-related neural region and reduce pain experience. Proc. Natl. Acad. Sci. 108, 11721–11726.
18.
19. Fung, B.J., Qi, S., Hassabis, D., Daw, N., and Mobbs, D. (2019). Slow escape decisions are swayed by trait anxiety. Nat. Hum. Behav. 3, 702–708.
20. Grupe, D.W., and Nitschke, J.B. (2013). Uncertainty and anticipation in anxiety: an integrated neurobiological and psychological perspective. Nat. Rev. Neurosci. 14, 488–501.
21. Harrison, B.J., Fullana, M.A., Via, E., Soriano-Mas, C., Vervliet, B., Martínez-Zalacaín, I., Pujol, J., Davey, C.G., Kircher, T., Straube, B., et al. (2017). Human ventromedial prefrontal cortex and the positive affective processing of safety signals. NeuroImage 152, 12–18.
22. Hassabis, D., Kumaran, D., Vann, S.D., and Maguire, E.A. (2007). Patients with hippocampal amnesia cannot imagine new experiences. Proc. Natl. Acad. Sci. 104, 1726–1731.

559 23. Ii, T.C.R., and Lima, S.L. (2006). PREDATORY BEHAVIOR AND DIET OF WINTERING
560 MALE COOPER'S HAWKS IN A RURAL HABITAT. J. Raptor Res. 40, 287–290.
561 24. Iigaya, K., Hauser, T.U., Kurth-Nelson, Z., O'Doherty, J.P., Dayan, P., and Dolan, R.J. (2019).
562 The value of what's to come: neural mechanisms coupling prediction error and reward
563 anticipation. BioRxiv 588699.
564 25. Jocham, G., Klein, T.A., and Ullsperger, M. (2011). Dopamine-Mediated Reinforcement
565 Learning Signals in the Striatum and Ventromedial Prefrontal Cortex Underlie Value-Based
566 Choices. J. Neurosci. 31, 1606–1613.
567 26. Lau, B., and Glimcher, P.W. (2007). Action and Outcome Encoding in the Primate Caudate
568 Nucleus. J. Neurosci. 27, 14502–14514.
569 27. LeDoux, J.E., and Pine, D.S. (2016). Using Neuroscience to Help Understand Fear and Anxiety:
570 A Two-System Framework. Am. J. Psychiatry 173, 1083–1093.
571 28. Leong, Y.C., Radulescu, A., Daniel, R., DeWoskin, V., and Niv, Y. (2017). Dynamic Interaction
572 between Reinforcement Learning and Attention in Multidimensional Environments. Neuron 93,
573 451–463.
574 29. Lima, S.L. (1985). Maximizing feeding efficiency and minimizing time exposed to predators: a
575 trade-off in the black-capped chickadee. Oecologia 66, 60–67.
576 30. Lisman, J., and Redish, A. d. (2009). Prediction, sequences and the hippocampus. Philos. Trans.
577 R. Soc. B Biol. Sci. 364, 1193–1201.
578 31. Maren, S., and Quirk, G.J. (2004). Neuronal signalling of fear memory. Nat. Rev. Neurosci. 5,
579 844–852.
580 32. Martindale, S. (1982). Nest defense and central place foraging: A model and experiment. Behav.
581 Ecol. Sociobiol. 10, 85–89.
582 33. Miller, K.J., Botvinick, M.M., and Brody, C.D. (2017). Dorsal hippocampus contributes to
583 model-based planning. Nat. Neurosci. 20, 1269–1276.
584 34. Mobbs, D. (2018). The ethological deconstruction of fear(s). Curr. Opin. Behav. Sci. 24, 32–37.

585 35. Mobbs, D., and Kim, J.J. (2015). Neuroethological studies of fear, anxiety, and risky decision-
586 making in rodents and humans. Curr. Opin. Behav. Sci. 5, 8–15.
587 36. Mobbs, D., and LeDoux, J. (2018). Editorial overview: Survival behaviors and circuits. Curr.
588 Opin. Behav. Sci. 24, 168–171.
589 37. Mobbs, D., Petrovic, P., Marchant, J.L., Hassabis, D., Weiskopf, N., Seymour, B., Dolan, R.J.,
590 and Frith, C.D. (2007). When Fear Is Near: Threat Imminence Elicits Prefrontal-Periaqueductal
591 Gray Shifts in Humans. Science 317, 1079–1083.
592 38. Mobbs, D., Yu, R., Rowe, J.B., Eich, H., FeldmanHall, O., and Dalgleish, T. (2010). Neural
593 activity associated with monitoring the oscillating threat value of a tarantula. Proc. Natl. Acad.
594 Sci. 107, 20582–20586.
595 39. Mobbs, D., Hagan, C.C., Dalgleish, T., Silston, B., and PrÃ©vost, C. (2015). The ecology of
596 human fear: survival optimization and the nervous system. Front. Neurosci. 9.
597 40. Mobbs, D., Trimmer, P.C., Blumstein, D.T., and Dayan, P. (2018). Foraging for foundations in
598 decision neuroscience: insights from ethology. Nat. Rev. Neurosci. 19, 419–427.
599 41. Mobbs, D., Headley, D.B., Ding, W., and Dayan, P. (2020). Space, Time, and Fear: Survival
600 Computations along Defensive Circuits. Trends Cogn. Sci. 24, 228–241.
601 42. Nili, U., Goldberg, H., Weizman, A., and Dudai, Y. (2010). Fear thou not: activity of frontal and
602 temporal circuits in moments of real-life courage. Neuron 66, 949–962.
603 43. Norman, K.A., Polyn, S.M., Detre, G.J., and Haxby, J.V. (2006). Beyond mind-reading: multi-
604 voxel pattern analysis of fMRI data. Trends Cogn. Sci. 10, 424–430.
605 44. Padilla-Coreano, N., Bolkan, S.S., Pierce, G.M., Blackman, D.R., Hardin, W.D., Garcia-Garcia,
606 A.L., Spellman, T.J., and Gordon, J.A. (2016). Direct Ventral Hippocampal-Prefrontal Input Is
607 Required for Anxiety-Related Neural Activity and Behavior. Neuron 89, 857–866.
608 45. Price, J.L., and Drevets, W.C. (2010). Neurocircuitry of mood disorders. Neuropsychopharmacol.
609 Off. Publ. Am. Coll. Neuropsychopharmacol. 35, 192–216.

610 46. Qi, S., Hassabis, D., Sun, J., Guo, F., Daw, N., and Mobbs, D. (2018). How cognitive and
611 reactive fear circuits optimize escape decisions in humans. Proc. Natl. Acad. Sci. 115, 3186–
612 3191.
613 47. Sangha, S., Diehl, M.M., Bergstrom, H.C., and Drew, M.R. (2020). Know safety, no fear.
614 Neurosci. Biobehav. Rev. 108, 218–230.
615 48. Stachenfeld, K.L., Botvinick, M.M., and Gershman, S.J. (2017). The hippocampus as a predictive
616 map. Nat. Neurosci. 20, 1643–1653.
617 49. Wallis, C.U., Cardinal, R.N., Alexander, L., Roberts, A.C., and Clarke, H.F. (2017). Opposing
618 roles of primate areas 25 and 32 and their putative rodent homologs in the regulation of negative
619 emotion. Proc. Natl. Acad. Sci. U. S. A. 114, E4075–E4084.
620 50. Wetterer, J.K. (1989). Central place foraging theory: When load size affects travel time. Theor.
621 Popul. Biol. 36, 267–280.
622 51. Wilkinson, L.S., Humby, T., Killcross, A.S., Torres, E.M., Everitt, B.J., and Robbins, T.W.
623 (1998). Dissociations in dopamine release in medial prefrontal cortex and ventral striatum during
624 the acquisition and extinction of classical aversive conditioning in the rat: Dopamine and aversive
625 conditioning. Eur. J. Neurosci. 10, 1019–1026.
626 52. Xu, M., Xu, G., and Yang, Y. (2016). Neural Systems Underlying Emotional and Non-emotional
627 Interference Processing: An ALE Meta-Analysis of Functional Neuroimaging Studies. Front.
628 Behav. Neurosci. 10.

629

Figures

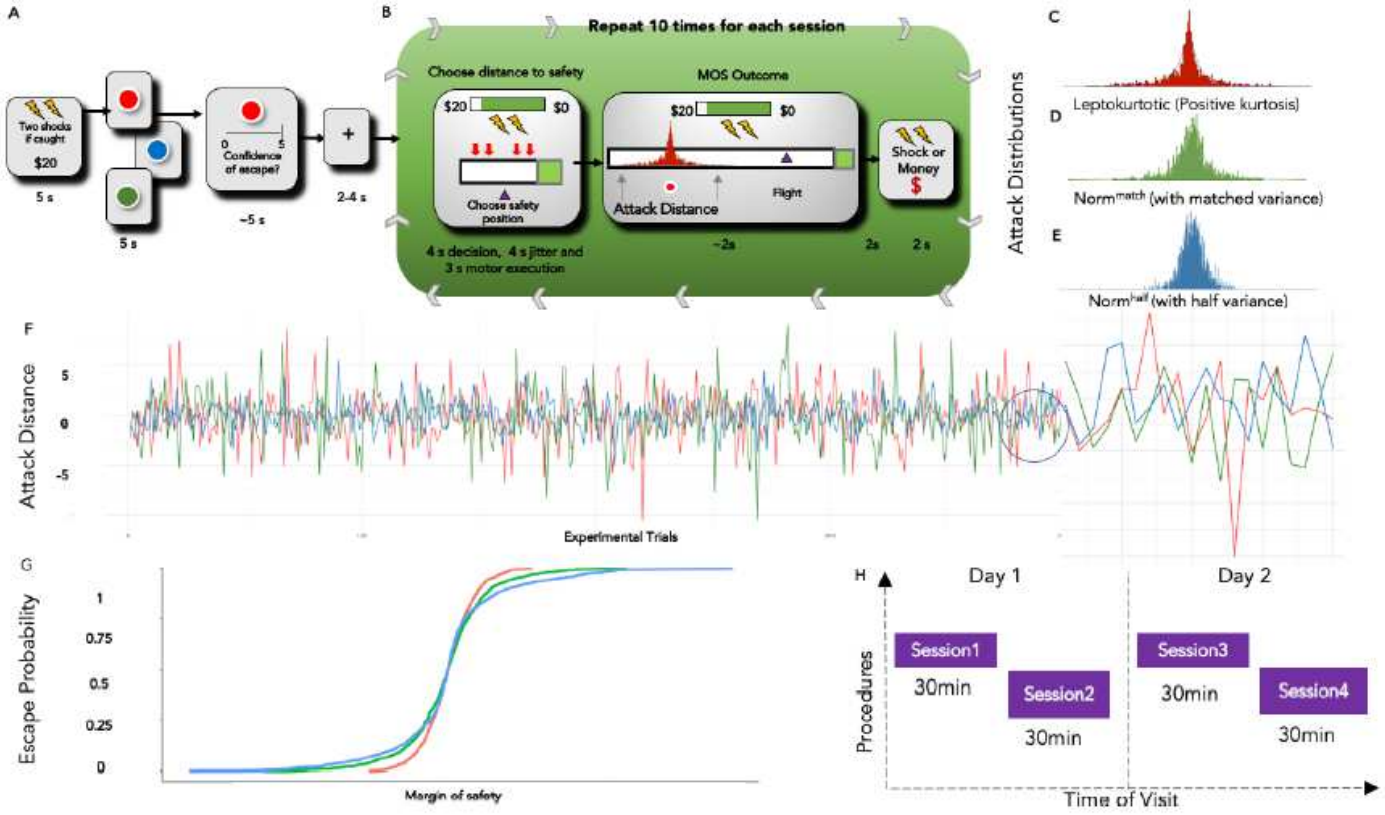

Figure 1

Experimental Structure

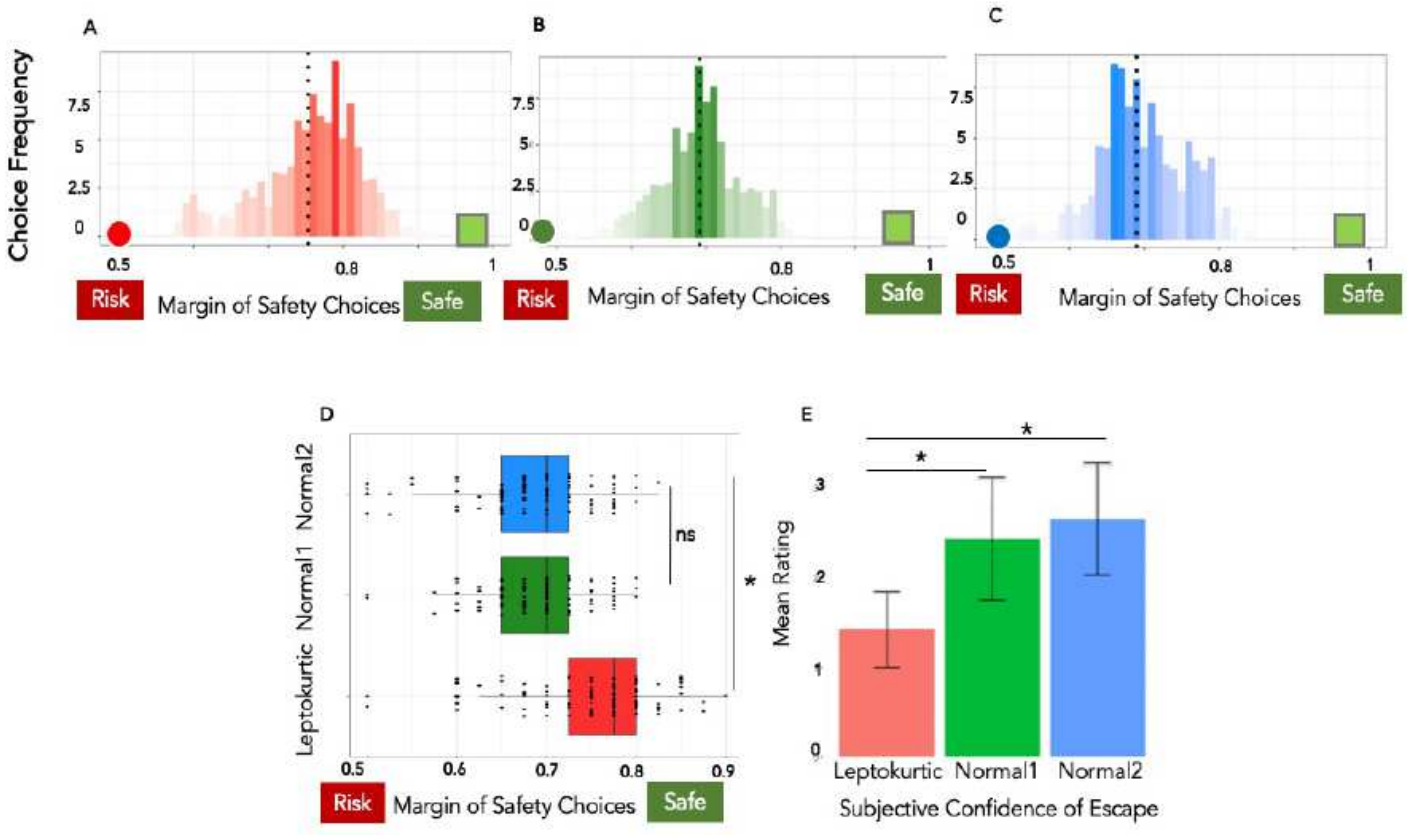

Figure 2

Behavioral Results

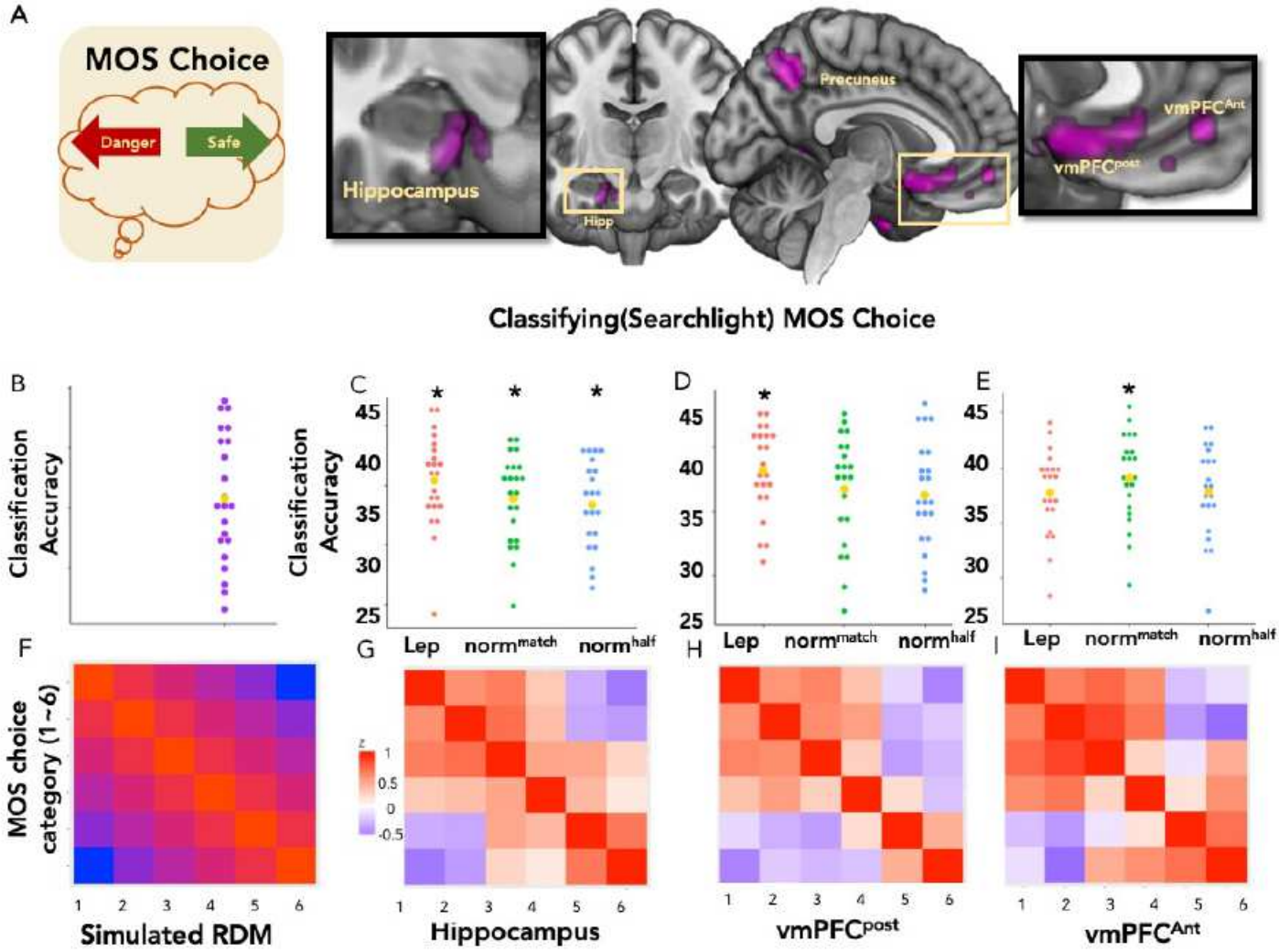

Figure 3

Neural representation of pre-emptive MOS decisions.

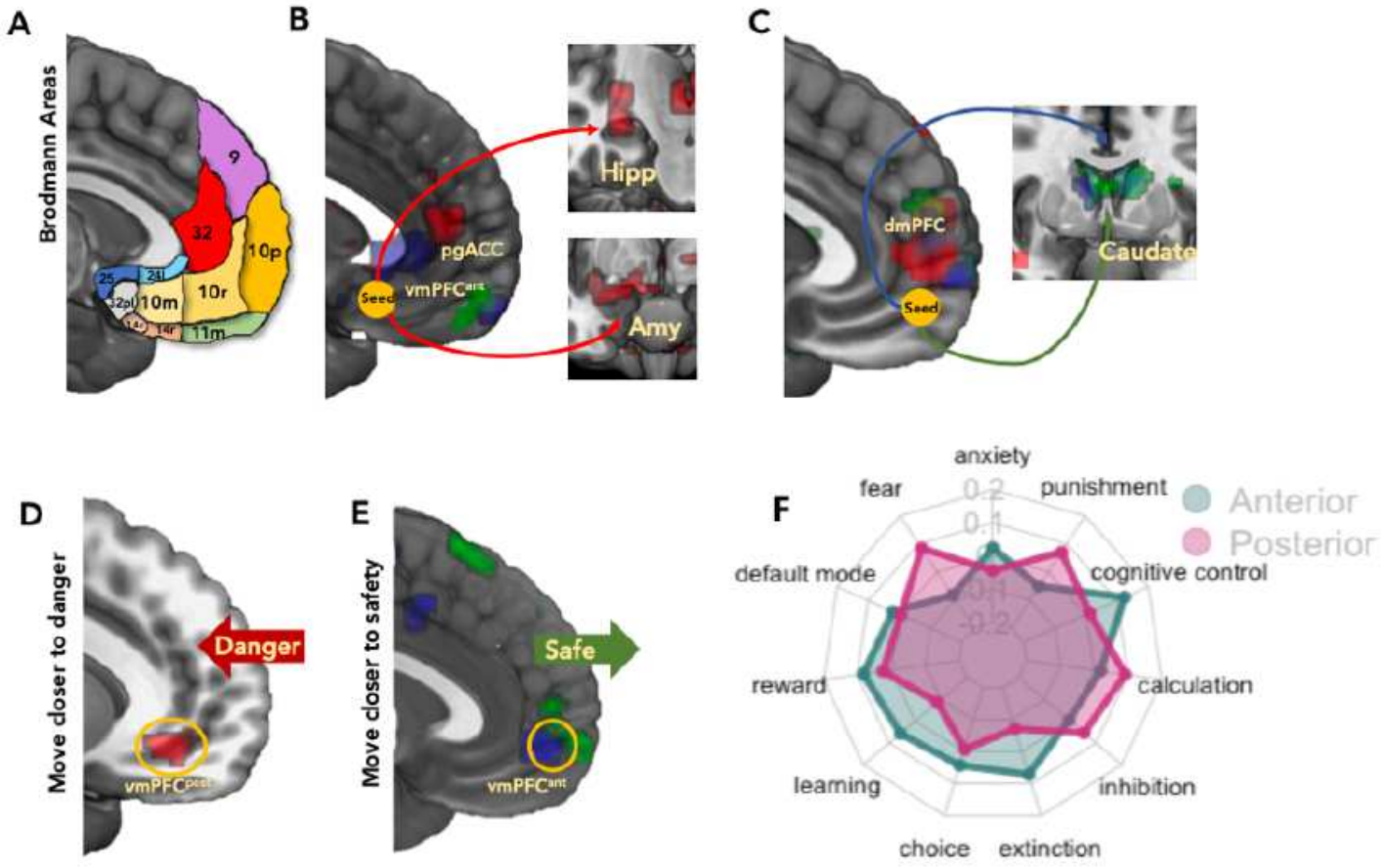

Figure 4

Psychophysiological interactions seeding from regions of interest and meta analytical decoding

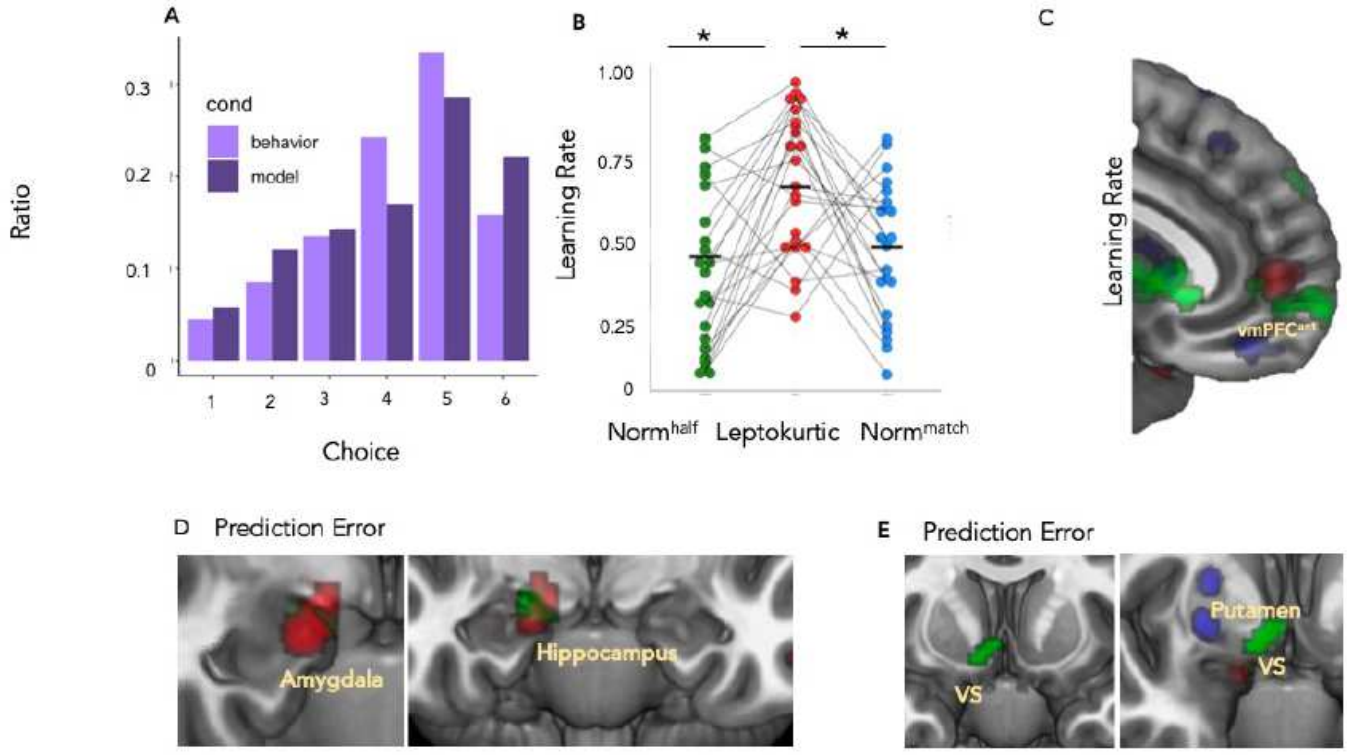

Figure 5

Behavioral modelling

Supplementary Files

This is a list of supplementary files associated with this preprint. Click to download.

- MOSSupplementaryMaterial.pdf